

Ambiguous figures and binding: EEG frequency modulations during multistable perception

WERNER EHM,^a MICHAEL BACH,^b AND JÜRGEN KORNMEIER^{a,b}

^aInstitute for Frontier Areas of Psychology and Mental Health, Freiburg, Germany

^bUniversitäts-Augenklinik, Freiburg, Germany

Abstract

Ambiguous figures induce sudden transitions between rivaling percepts. We investigated electroencephalogram frequency modulations of accompanying change-related de- and rebinding processes. Presenting the stimuli discontinuously, we synchronized perceptual reversals with stimulus onset, which served as a time reference for averaging. The resultant gain in temporal resolution revealed a sequence of time–frequency correlates of the reversal process. Most conspicuous was a transient right-hemispheric gamma modulation preceding endogenous reversals by at least 200 ms. No such modulation occurred with exogenously induced reversals of unambiguous stimulus variants. Post-onset components were delayed for ambiguous compared to unambiguous stimuli. The time course of oscillatory activity differed in several respects from predictions based on binding-related hypotheses. The gamma modulation preceding endogenous reversals may indicate an unstable brain state, ready to switch.

Descriptors: Binding problem, EEG, Gamma oscillation, Necker cube, Object perception, Temporal coding hypothesis

Research on multistable perception phenomena dates back to Necker's initial paper (Necker, 1832). However, the neural processes underlying spontaneous perceptual reversals remain elusive (for reviews, see Blake & Logothetis, 2002; Long & Toppino, 2004). A better understanding of how the perceptual system changes spontaneously between two different representations of the same visual object could also shed light on another more general issue, the binding problem: How, in principle, does the brain integrate separately analyzed features to a coherent object representation (e.g., Livingstone & Hubel, 1988; Treisman & Gormican, 1988; Uhlhaas et al., 2009)? In the last two decades binding type problems have also been discussed in connection with the grouping of letters of a word or words within a sentence, with the match of memory contents and perceptual contents, with sensory-motor coupling, the dynamic integration of distant neural subsystems, and with learning and consciousness (e.g., Cosmelli et al., 2004; Herrmann, Munk, & Engel, 2004; Revonsuo, 1999; Uhlhaas et al., 2009).

A widely favored but also criticized (e.g., Shadlen & Movshon, 1999) approach to the resolution of “the” binding problem relies on the temporal aspects of neural activity. It is hypothesized that neurons engaged in a common task such as the perceptual representation of some visual object are coordinated and grouped together through temporally synchronized rhythmic firing (Engel, Fries, Konig, Brecht, & Singer, 1999; Milner, 1974; von der Malsburg, 1981). This concept received support from studies with single cell recordings in animals (Eckhorn et al., 1988; Fries, Roelfsema,

Engel, Konig, & Singer, 1997; Gray, Konig, Engel, & Singer, 1989; Hirabayashi & Miyashita, 2005) and in humans (e.g., Tallon-Baudry, Bertrand, Henaff, Isnard, & Fischer, 2005).

A version of the temporal coding hypothesis applicable to electroencephalogram (EEG) data was proposed by Tallon-Baudry and Bertrand (1999). According to their “representational hypothesis,” induced gamma band activity (iGBA; cf. Data Analysis) should play an important role in object representation: Characteristic iGBA modulations would accompany the formation and decay of a coherent percept and reflect, for example, the binding of spatially restricted bottom-up neural activity related to the visual input and top-down activity like rehearsal, retrieval, and utilization of an internal (memorized) representation (e.g., Herrmann et al., 2004; Lutzenberger, Pulvermuller, Elbert, & Birbaumer, 1995; for a review, see Tallon-Baudry, 2009).

Spontaneous perceptual alternations in the absence of an external stimulus change should provide ideal test cases for the binding-by-synchrony/temporal coding and the related representational hypotheses (Borisjuk, Chik, & Kazanovich, 2009; Doesburg, Kitajo, & Ward, 2005; Engel et al., 1999; Engel, Fries, & Singer, 2001; Revonsuo, 1999; Tallon-Baudry & Bertrand, 1999; Varela, Lachaux, Rodriguez, & Martinerie, 2001). This is because such alternations should be accompanied by de- and rebinding processes and thus by changes in neural synchronization of a purely endogenous origin free from the confounding factors inevitable when the physical stimulus is changed.

Research was supported by grants from the Deutsche Forschungsgemeinschaft (BA 877-16).

Address correspondence to: Jürgen Kornmeier, Institute for Frontier Areas of Psychology and Mental Health, Wilhelmstraße 3a, 79098 Freiburg, Germany. E-mail: kornmeier@igpp.de

Ambiguous Figures, EEG Oscillations, and the Time Reference Problem

Perceptual reversals of ambiguous figures have been reported to be associated with a transient increase of (anterior right

hemispheric) gamma oscillatory activity (Başar-Eroglu, Strüber, Schürmann, Stadler, & Başar, 1996; Mathes, Struber, Stadler, & Basar-Eroglu, 2006; Strüber, Basar-Eroglu, Hoff, & Stadler, 2000; Strüber, Basar-Eroglu, Miener, & Stadler, 2001), a concurrent decrease of alpha activity, and a P300-like positive event-related potential (ERP) component (İşoğlu-Alkaç et al., 2000; Strüber & Herrmann, 2002).

A major problem with endogenous perceptual reversals is the lack of a suitable time reference for the not directly accessible reversal instant (Keil, Muller, Ray, Gruber, & Elbert, 1999; Kornmeier & Bach, 2004; Strüber & Herrmann, 2002). Most of the above mentioned studies used the participant's manual response for this purpose. However, the intra-individual temporal jitter of the reaction times makes it difficult to identify a physiological signature as pre-, peri-, or post-reversal, complicating the interpretation of the reported effects. Stimulus presentation events as time reference were used by Keil et al. and Muller, Federspiel, Fallgatter, and Strik (1999). The former group found reversal-related gamma modulation but could not clarify whether it precedes or follows the reversal. The latter group reported reversal-related modulations in the delta and alpha frequency ranges but did not analyze higher frequencies. Unambiguous stimuli for comparison purposes were considered in neither of the two studies.

Recently Kornmeier et al. (Kornmeier & Bach, 2004; Kornmeier, Heinrich, Atmanspacher, & Bach, 2001) proposed another approach to the time reference problem applicable to any type of ambiguous figure. They drew upon Orbach, Ehrlich, and Heath's (1963) and Orbach, Zucker, and Olson's (1966) indication that presenting the Necker cube discontinuously with short interruptions should urge the reversal instant into a definite temporal relation with, and close to, stimulus onset. Kornmeier and Bach (2005) adopted this presentation mode and used the stimulus onset as time reference for averaging EEG trials. They reported an improved precision of this time reference with regard to the reversal instant (± 30 ms; Kornmeier & Bach, 2005) compared to reaction time (± 100 ms; Kornmeier & Bach, 2004). This also improved the temporal resolution of the underlying processes and allowed them to identify a chain of successive ERP components.

In the present article, the gain in temporal precision is utilized to reliably distinguish, for the first time, pre- and peri/post-reversal activity modulations in the frequency domain. This paves the way for testing some conceptions about binding and object representation related to the binding-by-synchrony and the representational hypotheses. Neural correlates of binding were most often reported for (and searched in) the gamma band, with a special focus on induced gamma activity (e.g., Roskies, 1999; Tallon-Baudry & Bertrand, 1999). Recent contributions to the temporal coding discussion also take lower frequencies into account (e.g., Fries, Nikolich, & Singer, 2007). Accordingly, we study amplitude modulations in the theta to beta bands in addition to the gamma band. Frequencies below 4 Hz (delta) would require longer analysis segments than the ones used here and are not considered. The data analyzed in the following is taken from Kornmeier and Bach (2004).

Methods

Participants

Sixteen participants (aged 20 to 31 years, 9 women, 7 men) with normal or corrected visual acuity took part in the experiment.

They gave informed written consent to participate and were naïve as to the specific experimental question. The experiments were performed in accordance with the ethical standards laid out in the Declaration of Helsinki (World Medical Association, 2000) and approved by the local review board.

Stimuli

Stimuli were perceptually ambiguous Necker lattices (a combination of nine Necker cubes; Figure 1c,d) and unambiguous variants with depth cues (shading, central perspective, OpenGL lighting model; Woo, Neider, & Davis, 1998) related to the two possible three-dimensional (3D) interpretations of the Necker lattices (Figure 1a,b). All stimuli were generated with a Macintosh G4 computer and presented on a Philips GD 402 monochrome monitor with a frame rate of 85 Hz under a viewing angle of $7.51^\circ \times 7.51^\circ$. Luminance of the Necker lattice was 20 cd/m^2 ; luminance of the unambiguous lattices was 20 cd/m^2 averaged across all vertices. In all experimental blocks, successive stimuli were jittered in 3D space over $\pm 12^\circ$ of both elevation and azimuth angle, resulting altogether in 14 unambiguous and 7 ambiguous variants, thus avoiding afterimages as trivial local cues. A small cross in the center of the screen served as a fixation target.

EEG Recording

EEG was recorded from nine gold-cup scalp electrodes at Oz, P3, P4, Pz, C3, C4, Cz, Fz, and FPz (American Clinical Neurophysiology Society, 2006), with averaged ears as reference. Vertical electrooculogram (EOG) electrodes controlled for eyeblinks. Signals were amplified, filtered (first-order analog pass bandpass 0.3–70 Hz), digitized with a resolution of 12 bits at a sampling rate of 500 Hz, and streamed to disk.

Procedure

The Necker lattice is a two-dimensional projection of a 3D object. When viewed binocularly, a conflict arises between the 3D interpretation and the missing stereo disparity. Participants viewed the stimuli monocularly in order to prevent such a conflict. We ran two experiments, one with the ambiguous Necker lattices, the other one with the unambiguous lattices. In each experiment the stimuli were presented discontinuously, an 800-ms presentation interval alternating with a 400-ms interstimulus interval (ISI) showing a blank screen. After ambiguity of the Necker stimuli was pointed out to the participants, they compared in a go/no-go task the perceived front–back orientation of the current stimulus with that of the preceding one in two experimental conditions. In one condition they pressed a key whenever the currently perceived orientation differed from the preceding one (reversal condition [RC]). The second condition was identical except that the task was the opposite: a key press whenever the perceived orientation of the stimulus remained the same (stability condition [SC]). Each key press, which had to be executed in the ISI following the task-relevant event, extended that ISI to 1000 ms and terminated the current trial. The first stimulus thereafter started the next trial, which again lasted until the next key press. A trial thus consisted of several (at least two) ISI+presentation interval pairs hereafter called segments. Because of the go/no-go paradigm, the number of such segments varied from trial to trial. The average number of segments within a trial differed also between conditions and stimuli. For instance, a trial usually included more segments (hence lasted longer) under condition RC than under SC, because a percept

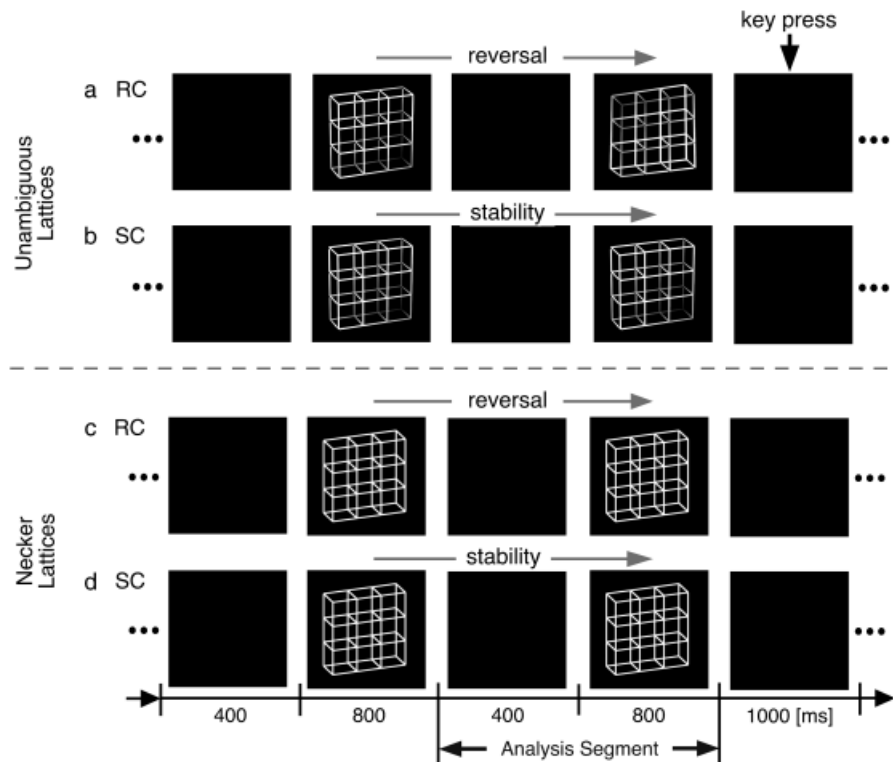


Figure 1. Paradigm. Participants viewed in different experiments either unambiguous lattices (a,b) or ambiguous lattices (c,d) and compared the 3D perspective of successively presented stimuli. In separate experimental conditions they indicated in a go/no-go manner either a perceived perspective reversal (conditions RC in a and c) or perceived stability (conditions SC in b and d) across two successive stimulus presentations by a key press in the ISI following the respective perceptual event. Each key press extended the current ISI from 400 ms to 1000 ms.

reversal across two successive presentations was less likely than percept stability.

In each of the four experiment–condition combinations, trials came in six blocks, with a break of about 1 min in between. Usually, a block was terminated after either 20 responses or 7 min duration. For a few participants with many artifacts or low reversal rate, block length was prolonged in order to get roughly 100 artifact-free trials (see below) per experiment and condition. The $2 \times 2 \times 6 = 24$ blocks were counterbalanced across experiments and conditions in an ABCDDCBA scheme in order to reduce sequential effects. The entire experimental session lasted about 3 h with a break of about 10 min after half of the time.

Our design disentangles trial epochs from task execution and motor activity. Furthermore, it introduces the stability condition as a suitable control for the reversal condition. In the latter, participants were instructed to report reversals only if they occurred with stimulus onset and to ignore reversals (if any) occurring later in the presentation interval. They reported after the experiment that such delayed reversals happened never or very rarely.

Data Analysis

EEG recordings were split into trials (cf. Procedure), and an analysis segment was chosen within each trial. The analysis segment consisted of the *last* (800 ms) presentation interval before a key press along with the (400 ms) interstimulus interval preceding it. The instant of stimulus onset in an analysis segment was chosen as the common time reference across trials, $t = 0$. Because endogenous perceptual reversals might be initiated earlier than

400 ms before stimulus onset, we occasionally also considered extended analysis segments reaching from 1600 ms before to 800 ms past $t = 0$. Analysis segments showing amplitude excursions exceeding $\pm 100 \mu\text{V}$, typically related to blinks or eye movements, were automatically detected and discarded, along with the whole trial containing that segment. The minimum number of artifact-free analysis segments per participant, experiment, and condition was 64, the maximum 171, the average 113.1.

We then computed the short time Fourier transform (STFT) across each artifact-free analysis segment, using a Hanning window (Papoulis, 1962) with four different window widths. The selected window widths were 160, 240, 320, and 480 ms, to be applied with different frequency ranges corresponding to 40–65 (upper gamma), 26–40 (lower gamma), 14–26 (beta), and 4–14 Hz (theta to alpha), respectively. The time region actually analyzed was restricted to the interval $[-240, 480]$ ms in order to minimize boundary effects and because “late” components were not in our focus.

Based on the single trial STFTs, a three-level hierarchy of (event-related) time–frequency charts (TFC) was defined as follows: (1) At the lowest level, for each subject, stimulus, experimental condition, electrode, and analysis segment, single trial time–frequency charts ($\text{TFC}_{\text{trial}}$) were obtained by taking absolute values of the respective STFT (amplitudes) and subtracting a frequency-specific baseline (more details below). (2) At the subject level, individual time–frequency charts (TFC_{subj}) were obtained by averaging the respective single-trial time–frequency charts across trials. (3) Finally, grand means of the individual time–frequency charts across participants yielded average time–frequency charts ($\text{TFC}_{\text{grand}}$).

For statistical testing, TFCs were compressed on the frequency axis and band-activity traces (BAT_{trial} , BAT_{subj} , BAT_{grand}) were obtained by averaging the respective TFCs across various frequency bands in the theta to gamma range. To remove the activity related to stimulus onset and the processing of low-level stimulus features, we focused on *differences* of TFCs/BATs under the reversal (test) and stability (control) conditions, namely, RC minus SC.

A note on terminology: The TFCs/BATs as computed here represent what is often called induced activity. We adhere to this usage even though some authors prefer to call it total activity (e.g., Herrmann et al., 2004). More important is the delimitation of induced/total activity from evoked activity, which is computed from the ERP rather than from single trials. Evoked activity picks up only those features that are strictly phase-locked, whereas the present induced measures also collect activity jittering in time across trials, as it typically occurs before stimulus onset and at higher latencies or in endogenously generated processes, which are of particular interest here.

Statistics

Under the null hypothesis H_0 , “no systematic difference between the reversal condition (RC) and the stability condition (SC),” the time course of the difference of the respective band activity traces should only exhibit chance fluctuations around the zero line. Randomization tests were performed to check for systematic departures from H_0 at the population level.

The tests were based on the maximum and minimum values (separately) assumed by the difference of the average (= average of differences) traces $BAT_{\text{grand}}(\text{RC}) - BAT_{\text{grand}}(\text{SC})$ within a *time* region of interest (ROI). A reference null distribution for the observed extrema was obtained as follows. For each subject, the two BAT_{subj} under study were randomly labeled SC^* and RC^* . The difference $BAT_{\text{subj}}(\text{RC}^*) - BAT_{\text{subj}}(\text{SC}^*)$ was then averaged across participants, and the extreme values were obtained in the resulting average trace. This was repeated 10,000 times, providing reference distributions, hence p values, for the actually observed maximum and minimum values. Such a randomization procedure yields a correct p value up to a random error that is largely negligible with 10,000 repetitions (Edgington & Onghena, 2007).

To get a time-, frequency-, and space-resolved picture, the tests were carried out for a large number of (preselected) tfe cells: A tfe cell is understood as a triplet (T, F, E) resulting from the choice of a ROI T , a frequency band F , and an electrode E . ROIs T were chosen as overlapping time intervals of width 160 ms centered at delays $-80, 0, 80, \dots, 400$ ms with respect to stimulus onset. Frequency bands F in the range 4–65 Hz, such as 4–7 Hz, 8–13 Hz, and so forth, were selected jointly with suitable window widths of the STFT as indicated above.¹ A significant result for the maximum (minimum) type test at tfe cell (T, F, E)

¹Frequency bands F were selected by the following criteria. They should (1) sparsely cover the range from 4 to 65 Hz, (2) fall roughly within some standard frequency range, (3) be neither too large (to allow for sufficient discrimination) nor too narrow (compared to the actual frequency resolution), and (4) overlap (because a peak/dip at the boundary of F is difficult to detect with average amplitudes across F). Given these criteria, we decided to select the following frequency bands: 4–7; 8–13, 10–15; 14–20, 20–26, 14–26; 26–32, 32–40, 26–40; 40–50, 45–55, 50–60, 55–65; 35–55, 40–60, 45–65 Hz. It should be noted that the classical frequency bands (e.g., alpha: 8–12/13 Hz) refer to “raw” signals. However, which frequency bands are relevant to the comparison RC versus SC is not a priori clear.

indicates that the oscillatory activity for frequencies in band F at electrode E is distinctly higher (lower) somewhere within ROI T under the reversal than under the stability condition.

Analogous tests for comparisons a and b were applied at the level of individual participants, based on the maximum (and minimum) of the difference trace $BAT_{\text{subj}}(\text{RC}) - BAT_{\text{subj}}(\text{SC})$. Corresponding reference distributions were obtained similarly as above by shuffling the single trials. The trials from both conditions were pooled and then randomly reassigned to SC and RC, observing the original number of trials in the two conditions. Repeated 10,000 times, the procedure yielded a p value for the observed maximum as above, now at the individual level.

The choice of a baseline interval presents special problems in our case. Usually in studies with evoked potentials, the baseline is taken across a short time interval before stimulus onset. The exact choice was nonessential if “nothing of interest” happened within this baseline interval, as is usually assumed. With ambiguous stimuli, however, endogenous perceptual reversals may well be “prepared” prior to stimulus onset within the typical range of baseline intervals, so that effects of interest may be confounded with baseline adjustment effects.² To make significance criteria less dependent on the choice of the baseline, we considered three different baseline intervals, namely $[-100, 0]$, $[-200, 0]$, and $[-240, +480]$ ms, and reported as “three-significant” only those instances where the single tests were significant for all three baseline intervals simultaneously. Precisely, we considered as three-significant (***) any test for which all three p values are $< .01$; and as three-significant (*) any test for which all three p values are $< .05$ and $p < .01$ for at least one of the baseline intervals.

We corroborated some results using a work-around for the baseline interval problem: the derivative, or increment, of a band activity trace with respect to time is independent of the baseline interval. Because local maxima of a trace are preceded (or followed) by maxima (or minima) of the derivative, the latter gives a clue to the onset (or offset) of a positive deflection of the trace, which can be of interest in itself. Tests for extrema of derivative traces were implemented in complete analogy to those for the original traces.

Alpha error inflation due to the massive multiple testing involved was only accounted for by setting tight limits via the notion of three-significance. Arguments defending such an exploratory approach are given in the discussion.

Results

Behavioral results (e.g., reversal rates) and ERPs for the present data have already been reported by Kornmeier and Bach (2004). Prior to our main results we first present, purely phenomenologically, the raw time-frequency characteristics of the original EEG response before differencing, which are also of interest.

Raw TFCs and BATs

Grand average TFCs averaged across the experimental conditions (indication of perceptual reversal and stability) are shown in Figure 2a, separately for the two stimuli (ambiguous [A] and unambiguous [U]). The most conspicuous patterns common to both stimuli are (a) the initial activation in the alpha to beta range

²The choice of the baseline interval determines what counts as a positive or negative deflection. For example, if the baseline interval is located around the global minimum of the trace, anywhere else one will find positive deflections.

immediately after onset that quickly shifts to and then persists in the theta and lower alpha range (<10 Hz); (b) the sustained deactivation in the beta band starting about 100 ms after onset at 20 Hz and afterward spreading to the whole beta and upper alpha band (10–26 Hz); (c) the less pronounced, transient increase in gamma activity (50 Hz) roughly around 350 ms after onset at the frontopolar electrode (FPz); and (d) a fourth feature, not so obvious from Figure 2a, that is a transient enhancement of gamma activity within the ISI before onset.

Remarkably, this pre-onset gamma enhancement essentially is confined to the ambiguous stimulus and to central and right-hemispheric electrode positions. As another difference, the post-onset gamma enhancement (feature c) apparently is delayed for ambiguous compared to unambiguous stimuli.

Further interesting phenomena become visible when epochs are prolonged to the “past” beyond the ISI; see Figure 3. For ease of reference, let us call the intervals [−400, 600] ms and [−1400, −400] ms the last and the penultimate segments before the key press, abbreviated LS and PS, respectively. Alpha and beta band traces clearly exhibit deactivation with time, in a two-fold sense. First, activity steeply goes down within both PS and

LS after a short ascent around the respective stimulus onset (which is at −1200 ms in PS) and then recovers steadily, though without returning to its initial level. Second, on a larger time scale, average amplitudes in the segment LS are distinctly decreased compared to those in the segment PS. In the theta band, activity strongly increases with stimulus onset and settles back roughly to its baseline after about 600 ms within both PS and LS. Gamma band traces exhibit more complex features (Figure 3, first three rows). Similar to the adjacent beta frequencies, there appears to be a tendency for gamma deactivation at a larger scale (i.e., across PS and LS). However, shapes differ from the staircase-like decrease in the alpha and beta bands and appear less homogeneous across conditions, stimuli, frequency bands, and electrodes.

Comparison of Experimental Conditions RC versus SC

The difference-TFC_{grand} in Figure 2b highlight the time-frequency regions of higher or lower activity under RC compared to SC. To single out the statistically significant excursions, tests based on maximal deflections of difference-BAT_{grand} were carried out for a large number of tfe cells covering the time-

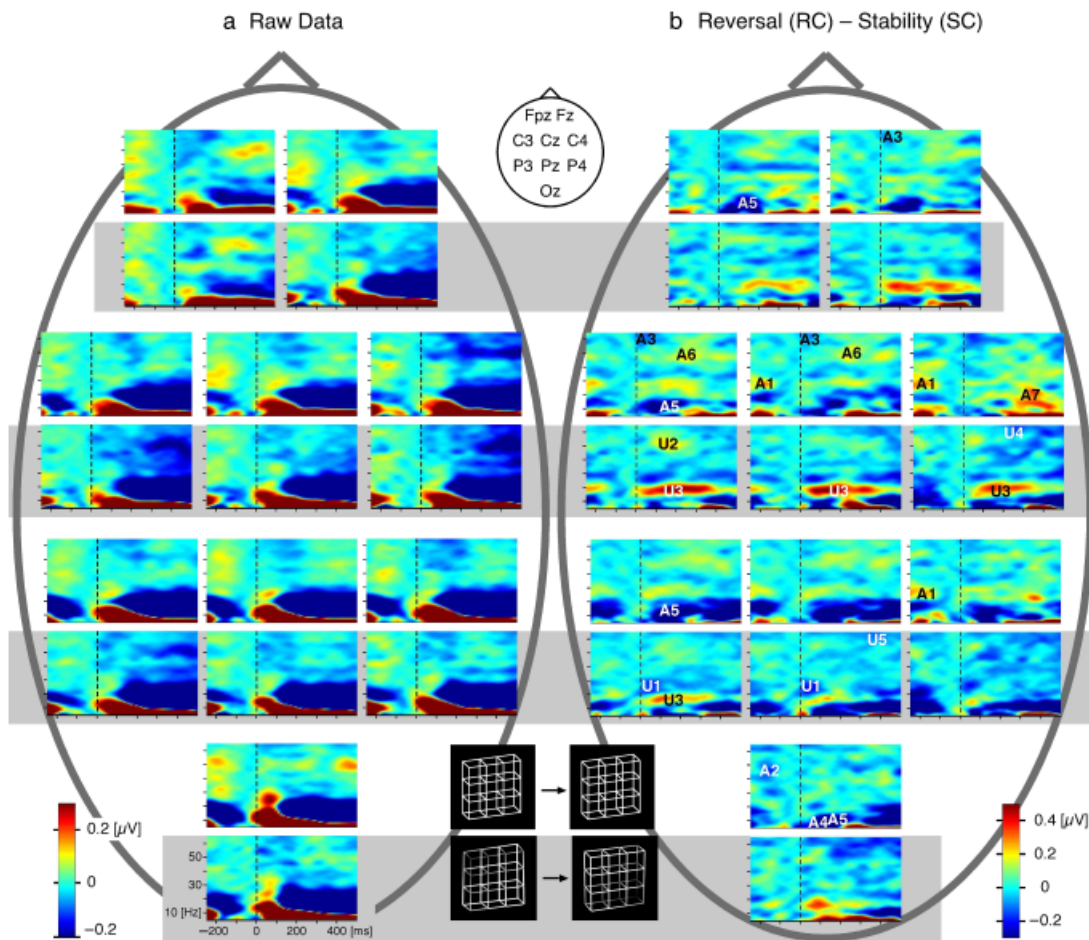


Figure 2. Time–frequency charts. The baseline interval was [−100,0] ms. The color scale in panel a was chosen so as to emphasize small effects at higher frequencies, which otherwise were unnoticeable due to dominance of low frequency amplitudes. (Conversely, modulations within large effects at low frequencies become less distinguishable.) Dashed vertical lines mark the stimulus onset. TFCs for the ambiguous and unambiguous stimuli are stacked in pairs, ambiguous on top, unambiguous underneath, on a gray background. (a) Raw time–frequency charts. Grand mean time–frequency charts were obtained by averaging TFC_{grand} (cf. Data Analysis) across conditions and stimuli. (b) Differences of TFC_{grand} (reversal minus stability). Entries in b such as A1, U2, and so forth indicate the position in the time–frequency plane of significant deflections from zero (“components”; cf. Table 1). A: ambiguous; U: unambiguous; 1, 2, and so forth: temporal order; black/white coloring of the numbers and letters is only for saliency.

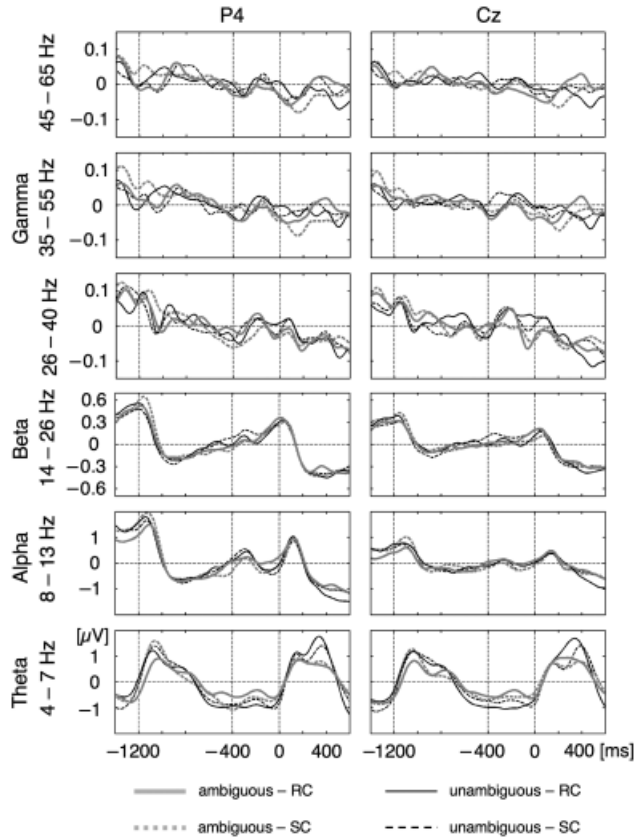


Figure 3. Band activity traces BAT_{grand} were obtained by averaging time–frequency charts TFC_{grand} over selected frequency bands. Solid and dashed lines stand for reversal and stability conditions, respectively, and gray-bold and black-thin for ambiguous and unambiguous stimuli, respectively. For presentation, traces were baseline corrected by subtracting average amplitudes.

frequency–electrode space (cf. Statistics). Table 1 lists all the cells that gave rise to a three-significant test result for the ambiguous stimulus, ordered according to peak time and grouped into components. Such listings, followed by a grouping according to peak time, frequency, and sign, underlie all features discussed in the following. For frequencies below or above 26 Hz, significance is understood as three-significant (**) or three-significant (*), respectively. Only the cells with ROIs ending not later than 400 ms after onset are taken into account.

In Figure 2b the significant components are indicated by numbers in the order of their appearance, accompanied by prefix A (ambiguous) in order to distinguish them from components U1, U2, and so on found with stimulus U (unambiguous). For the latter, components were obtained in the same way as for stimulus A, based on a list of three-significant test results. The difference charts represent grand means without any information about the variability across participants. Thus what appears prominent in Figure 2b need not necessarily be significant, nor do all significant components stand out clearly.

Figure 4 summarizes the test results by indicating peak times, frequencies, positions, and signs of the components. The most conspicuous difference between stimuli A and U is the appearance of components A1 and A2 within the ISI before stimulus onset in the case of stimulus A. This pattern of activity has no counterpart with stimulus U, which underlines a similar obser-

Table 1. Listings of All Three-Significant Outcomes When Testing RC versus SC (Necker Stimulus)

ROI (ms)	Frequency band (Hz)	Electrode	Extremum		
			Peak time (ms)	Sign	Component
[−240, −80]	26–32	P4	< −250	+	A1
[−160, 0]		C4	−160		
[−240, −80]		Cz	−178		
[−240, −80]	40–50	Oz	−166	−	A2
[−160, 0]			−158		
[−160, 0]	35–55		−166		
[−80, 80]	55–65	C3	26	−	A3
[0, 160]			26		
[−80, 80]		Cz	34		
[−80, 80]		Fz	34		
[−80, 80]	4–7	Oz	74	−	A4
[0, 160]			74		
[0, 160]	8–13	P3	134	−	A5
[80, 240]			134		
[0, 160]	10–15	Fpz	134		
[80, 240]			134		
[0, 160]	8–13	Oz	146		
[80, 240]			146		
[0, 160]	10–15	Fpz	146		
[80, 240]			146		
[0, 160]		P3	158		
[80, 240]			158		
[160, 320]			170		
[160, 320]		C3	170		
[80, 240]		P3	194		
[160, 320]			194		
[160, 320]		C3	194		
[240, 400]	45–55	C3	258	+	A6
[240, 400]		Cz	242		
[240, 400]	35–55	Cz	250		
[240, 400]	14–26	C4	338	+	A7

Note: In columns 2 to 6, any entry identical to the one above it is omitted for better readability.

vation made for the raw TFCs (feature d in the previous section). Component A1 represents a positive deflection of the difference- BAT_{grand} at low gamma frequencies (26–32 Hz) about 200 ms before onset at right posterior and central positions. As a further check of the genuineness of the deflection, permutation tests for the derivatives of the difference traces were carried out (cf. Statistics). They resulted in significant ($p < .01$) minima at electrodes C4 and Cz for ROIs [−240, −80], [−160, 0], and band 26–32 Hz located about 130 ms before onset, that is, in the right flank of the peak of the original difference traces. No significant maxima of derivatives were found in the left flank, maybe due to a less rapid ascent to the maximum than decay from it. Components A1, A2 are followed by a succession of three negative deflections starting immediately after onset at left central and frontal positions in the high gamma range (A3), and ending after about 200 ms at left hemispheric positions with frequencies in the range 8–15 Hz (A5). Differential gamma reduction early after stimulus onset also is observable for the unambiguous stimulus (U1), whereas the latter two features (A4 and A5) occur with ambiguous figures only. A feature shared by both stimuli is the positive higher gamma deflection at left central electrodes and 150 to 250 ms peak time (components A6, U2). In both cases it is followed by a positive deflection in the beta band (components A7, U3; see the gray underlain areas in Figure 4). However, there is a marked difference in the peak time of the components

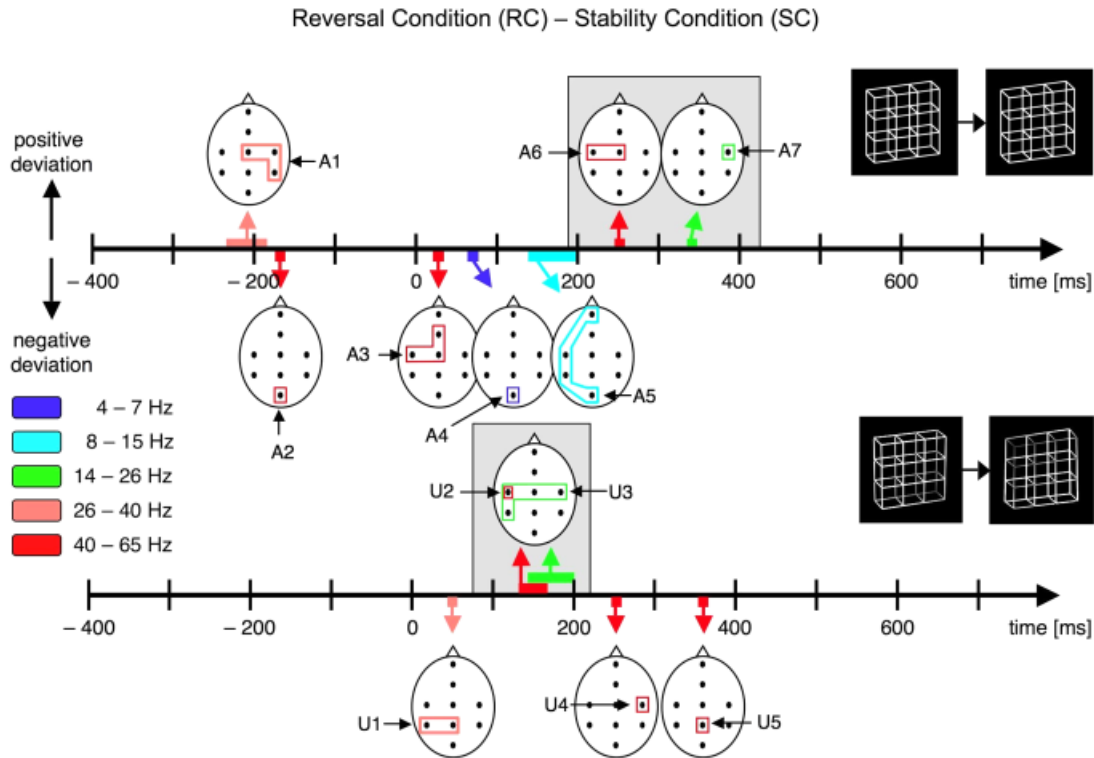


Figure 4. Significance diagram: Summary of all significant differences (“components” in Table 1). The closed polygons surrounding electrodes mark three-significant test results; color indicates the corresponding frequency range. Head positions on the time axes indicate peak time. Positive (negative) excursions appear above (below) the time axes. Top: Necker stimulus; bottom: unambiguous stimulus. Gray backgrounds highlight apparent analogies between ambiguous and unambiguous stimuli.

between stimuli, those for A being delayed by about 100 ms compared to U.

Individual versus Group Results

Tests on the participant level were carried out only for the cells relevant to the components identified in the group analysis. Interindividual variability was considered by allowing for slightly more flexibility regarding frequency bands if these appeared too narrow. For instance, component A1 was taken to consist of its deviation type (positive) together with all the cells obtained by free combinations of ROI [−240, −80] ms, bands 26–32, 26–40 Hz, and electrodes P4, C4, Cz. Table 2 summarizes the individual test results by listing for each component the number of participants having a three-significant outcome for at least one of the relevant tfe cells. The term three-significance here is understood in a weakened sense: (*) and (**) mean that $p < .05$ and $p < .02$ for all three baselines, respectively.

Discussion

Ambiguous figures allow for the investigation of EEG correlates of the decay and rebuilding of object representations in the absence of potentially confounding factors related to a change in visual stimulation. In the present study, we analyzed EEG correlates of spontaneous perceptual reversals of a Necker-type stimulus in the time–frequency domain. Using a discontinuous stimulus presentation mode, we synchronized perceptual reversals with stimulus onset and used the latter as a time reference for the reversal instant. Participants continually compared the perceived stimulus perspective between successive presentations. In two experimental conditions of the go/no-go type, they had to

indicate either perceptual reversal (reversal condition) or perceptual stability (stability condition). A second, entirely analogous experiment was run with unambiguous stimulus variants. There, the orientation reversals were induced by the stimulation program.

This paradigm has a number of advantages. (1) The parallel consideration of an experiment with unambiguous stimuli allows for the identification of effects distinctive of endogenously generated percept reversals as compared to exogenously driven reversals. (2) Both experimental conditions, RC and SC, have identical stimulation protocols, use the same stimulus, and require preparation of a motor response. Therefore, EEG patterns related to such confounding factors should cancel when taking differences RC minus SC, and only the reversal-related activity should remain. Nevertheless, we also considered raw data before subtraction for better comparability with related EEG studies in which one or several confounders had not been, or could not be, handled symmetrically in the test (here: RC) and control (here: SC) conditions. (3) The discontinuous presentation paradigm yields a time reference, stimulus onset, that is more closely aligned to the reversal-related processes than a key press, the time reference commonly used with continuous presentation paradigms. Kornmeier and Bach (2006) reported a gain in temporal precision by a factor of more than 3, which helped uncover activity patterns that would otherwise be blurred by reaction time jitter. In particular, pre- and peri-/post-reversal events could be distinguished more reliably.

The present approach also has its limitations and challenges. (i) Our results do not immediately carry over to the case where the stimulus is observed continuously. Still, there is some evidence that, in regard to the spontaneous reversal-related

Table 2. Summary of the Individually Three-Significant Test Results

	Component											
	A1	A2	A3	A4	A5	A6	A7	U1	U2	U3	U4	
No. of participants	4	1	1	1	2	3	0	1	3	0	0	
Significance	*	*	*	**	**	*		*	**			

* $p < .05$; ** $p < .01$.

processes, the difference between the two settings is not substantial (e.g., Kornmeier & Bach, 2004, 2006; Sterzer & Rees, 2008). (ii) By items 1–3 above, our approach opens up chances for uncovering so far inaccessible neural correlates. This, conversely, means that there is yet little knowledge about potential regions of interest. One is thus left with a large search space initially, which in turn suggests adopting an exploratory approach using heavy multiple testing. (3) Any attempt to deal with the ensuing problem of alpha error inflation, for example, by means of (then necessarily massive) Bonferroni adjustment, would require very small p values. These, however are out of reach with the randomization tests used here.³ Given these considerations it appeared to us more important at the current stage to collect possibly meaningful patterns than to prove they are relevant. Ultimately, the latter question will not be answered by a single experiment but by accumulation of evidence from diverse studies under varied conditions.

We here report for the first time a sequence of time–frequency components tracking the processes underlying endogenous perceptual reversals of ambiguous figures with high temporal precision. This sequence has several similarities to but also important differences from the corresponding sequence for the experiment with unambiguous stimulus variants.

Raw time-frequency characteristics (prior to differencing)

- Object presentation causes an initial amplitude increase in the alpha and beta frequency range (after stimulus onset) that quickly shifts to the lower alpha and theta band. Further, there is a massive, sustained beta reduction starting about 100 ms after stimulus onset.
- On a larger time scale, average amplitudes at alpha and beta frequencies are decreased in the last interval before response compared to the penultimate stimulus interval.

These observations apply to both stimulus types and experimental conditions. Our main findings rely on test results for differences of band activity traces (BATs).

Differential time-frequency characteristics: Reversal minus stability

- Lower gamma activity (26–32 Hz) was (differentially) increased roughly about 200 ms before stimulus onset, which deflection was followed by a decrease of higher gamma activity (35–55 Hz) at about –160 ms. These

³Very small p values easily surviving Bonferroni correction are attainable with the classical F -type tests, but presuppose overreliance on distributional assumptions. Here, we applied randomization tests with guaranteed validity practically independent of preconditions. However, for the latter, it is often impossible to determine very small p values with the necessary accuracy because the required number of Monte Carlo simulations is infeasibly large.

transient modulations of the difference traces showed a right-hemispheric dominance and occurred with ambiguous Necker stimuli only. No prestimulus gamma modulation was observed in the case of exogenously induced reversals of unambiguous stimuli.

- For both stimulus types gamma band difference traces decreased shortly after stimulus onset.
- About 250 ms after stimulus onset, there was a transient increase of induced gamma activity for reversed compared to unchanged (stable) percepts in the case of ambiguous stimuli. A similar increase occurred about 100 ms earlier in the case of unambiguous stimuli. We associate it with what is commonly referred to as induced gamma band activity (e.g., Tallon-Baudry, 2009).

Could Gamma Activity Modulations Be Explained by Miniature Saccades?

In recent widely recognized studies, Yuval-Greenberg and Deouell (2009) and Yuval-Greenberg, Tomer, Keren, Nelken, and Deouell (2008) demonstrated that iGBA largely can be an artifact of a type of eye movement called miniature saccades. This fundamentally questions the origin of iGBA in gamma oscillations and, thus, its functional role in visual grouping and the related binding processes. We therefore checked whether miniature saccades could alternatively explain the present iGBA results. To summarize briefly, we found iGBA to be correlated with EEG spike clustering in the raw band activity traces (BAT_{subj}). Quantitatively, spike clustering was less strong than in Yuval-Greenberg et al.'s data. Moreover, the differential effects found when comparing the reversal and stability conditions were only marginally affected by spike rate modulations and less so for component A1 than for A6. Thus for our data, miniature saccades do not provide a sufficient explanation of these differential effects.

Neural Oscillations and Temporal Aspects of Binding

Our discussion will be organized around three predictions derived from the representational hypothesis (cf. Introduction). For clarity, let us state what, in the context of bistable perception of a Necker type stimulus, we tentatively considered as most relevant to binding: (i) the grouping of the single edges to a 3D object seen in a certain, well-defined perspective and (ii) the match of the incoming bottom-up sensory information with top-down memory contents (e.g., the memorized perspective of the stimulus).

Prediction 1: Onset of gamma activity when a new percept is built up. If iGBA reflects binding in the sense of (i) and (ii) above, the buildup of a new stable percept should be accompanied by an onset of enhanced iGBA (Tallon-Baudry, 2009; Uhlhaas et al., 2009). Based on previous ERP and reaction time findings we expect the onset of such activity to be delayed for endogenous as compared to exogenously induced reversals by about 40 ms (Kornmeier & Bach, 2006). In any case, it should antecede neural activity reflecting the maintenance of the newly built percept.

Enhancement of induced gamma activity at about 200–300 ms after stimulus onset of visual and auditory stimuli is an often reported finding. It was related to a variety of cognitive functions, often in connection with a binding interpretation (e.g., Engel et al., 2001; Herrmann et al., 2004; Tallon-Baudry & Bertrand, 1999; cf. Introduction) and recently also with miniature saccades (Yuval-Greenberg & Deouell, 2009; Yuval-Greenberg et al., 2008) as discussed above. For multistable perception,

enhancement of induced gamma activity during spontaneous perceptual reversals was observed in a number of studies (e.g., Başar-Eroglu et al., 1996; Mathes et al., 2006; Strüber et al., 2000, 2001); however, the timing of this activity with respect to the reversal instant remained vague. The higher temporal resolution achieved in the present study revealed two instances of a differential gamma modulation, located about 200 ms before and after the onset of a perceptually reversed Necker stimulus. It appears plausible to assume that binding as understood here does not start until the stimulus is presented, leaving only the post-onset gamma component as a possible correlate of binding. But how early or late is 200 ms in regard to binding?

The earliest ERP correlate of an endogenous perceptual reversal of a Necker stimulus found by Kornmeier and Bach (e.g., Kornmeier & Bach, 2006) was a positivity about 130 ms after stimulus onset (“reversal positivity”). The subsequent chain of ERP components was delayed by about 40 ms compared to an otherwise largely identical ERP chain found with exogenously induced reversals of unambiguous stimulus variants. Kornmeier and Bach argued that this processing delay should account for the time necessary to disambiguate the ambiguous visual information from the Necker stimulus and, furthermore, that the “decision” about the perceptual outcome had taken place 260 ms after stimulus onset, at the latest, which is the temporal position of the (ERP) “reversal negativity” (Britz, Landis, & Michel, 2009; Kornmeier & Bach, 2004, 2006; Pitts, Nerger, & Davis, 2007).

Let us, as in Kornmeier and Bach’s ERP analyses (e.g., Kornmeier & Bach, 2006), conceive of the succession of components displayed in Figure 4 as single steps of some underlying processing chain. Similarly here, the processing step underlying the iGBA enhancement occurs later with endogenously than with exogenously induced reversals (components A6, U2 in Figure 2b and Figure 4), and its temporal position at about 250 ms fits well with Kornmeier and Bach’s upper estimate for the completion of the perceptual decision process. The time delays, 100 ms here versus 40 ms in the ERPs, agree less well, which might partly be due to the lower temporal resolution of time–frequency analyses compared to ERPs. All in all, we may tentatively associate components A6 and U2 with Kornmeier et al.’s reversal negativity. Moreover, there might be a connection between the (hypothetical) disambiguation process starting at their reversal positivity and component A5. The temporal position of the reversal positivity, at 130 ms, coincides with the beginning of A5’s temporal extension (cf. Table 1). Along with A5’s broad spatial distribution, from occipital to frontopolar electrodes, and the fact that neither A5 nor the reversal positivity have an analogue with the unambiguous stimuli, this suggests associating component A5 with the disambiguation process involving recurrent activity between several brain areas.

We speculate that during disambiguation the perceptual system tries to match—or bind—the visual information to one of the perceptual interpretations (pre)existing in memory. Visual information may be called ambiguous if more than one interpretation is possible and a kind of binding competition takes place. This could explain the time delay of the measured ERP and frequency components between the ambiguous and unambiguous stimuli. The assumption that this kind of binding has already taken place at around 130 ms fits well with recent results by Kirchner and Thorpe (2006), who found that natural scenes with and without animals can be distinguished as early as 120 ms after stimulus onset. This would seem possible only if binding in the above sense has already taken place by that time.

According to these considerations, the transient gamma modulation (component A6) about 100 ms after the alpha modulation (component A5, between 130 ms and 190 ms) could mirror perceptual processes executing after disambiguation and, hence, after binding, in the sense described in connection with our predictions, has already been accomplished. This does not rule out a binding interpretation of component A6. It could reflect binding processes executing later on, such as binding necessary for a conscious percept or the binding of the perceptual outcome with the task and/or the related motor preparation and execution as recently suggested (Revonsuo, 1999; Uhlhaas et al., 2009). This, then, would mean that the processes from vision to action are implemented in a stepwise fashion, a supposition that would yet have to be verified. In any case, the discussion highlights the necessity of clearly specifying what is meant by “binding” when it comes to timing issues.

Prediction (2): Sustained gamma activity during perceptual stability. If iGBA reflects the maintenance of a percept, it should continue during perceptually stable periods. Recent studies (e.g., Rolls, 2000; Sterzer & Rees, 2008) suggest that the neural activity underlying a stable object representation is maintained even when the stimulus is temporarily absent during short inter-stimulus intervals as used in the present paradigm.

We only found transient gamma modulations. This is in line with a number of studies reporting a transient iGBA increase between 200 ms and 300 ms after stimulus onset (e.g., Tallon-Baudry, 2009). Induced gamma band activity was often interpreted as evidence for binding processes (e.g., Uhlhaas et al., 2009). However, the question of how the result of this binding—the final object representation—is held active during the period of the observer’s object awareness remains largely unanswered. If gamma oscillations were crucial in that respect, they should continue during periods of percept stability. In fact, sustained gamma activity could be observed with single cell ablations in primates (e.g., Fries et al., 1997; Fries, Schroeder, Roelfsema, Singer, & Engel, 2002) and humans as well as in magnetoencephalography (MEG) data (e.g., Hoogenboom, Schoffelen, Oostenveld, Parkes, & Fries, 2006), though generally not with EEG data in humans (e.g., Tallon-Baudry et al., 2005); an exception is the study by Koch, Werner, Steinbrink, Fries, and Obrig (2009). In response to this issue, it was hypothesized that transient gamma in the EEG signifies the supposedly fast buildup of a coherent percept rather than its maintenance (e.g., Engel et al., 1999; Revonsuo, 1999; Uhlhaas et al., 2009). The question of how the percept is held active once built up was not addressed. According to another idea, gamma oscillations come in periodic bursts gated by low frequency oscillations (3–6 Hz) during periods of percept stability (Fries et al., 2007; see also Schroeder & Lakatos, 2009). The object representation would then be maintained by continued refreshment or cognitive update (e.g., VanRullen, Reddy, & Koch, 2006). A third possibility might result from too fuzzy a time reference. Even if gamma oscillations were sustained during the period of percept stability, that period could be shifted back and forth across trials relative to the time reference. Averaging across trials would then produce a peak in the center of the jitter region and, hence, the impression of a transient phenomenon. For stimulus-related activity, such is certainly more likely to happen when relying on a button press as a time reference than with the present paradigm.

In contrast to the gamma band, we did observe sustained activity modulations at lower frequencies. In large parts of the presentation intervals theta activity was enhanced, whereas beta

was suppressed in the TFC_{grand}/BAT_{grand} data before subtraction (Figures 2a and 3). In fact, a growing body of literature reports lower frequency oscillations correlated with several perceptual and cognitive brain functions (e.g., Gail, Brinksmeier, & Eckhorn, 2004; Klimesch, Freunberger, Sauseng, & Gruber, 2008; Pfurtscheller & Lopes da Silva, 1999). For example, there is recent evidence for sustained oscillations in the alpha range correlated with motion perception of the ambiguous Wagon-Wheel stimulus (VanRullen et al., 2006). This raises the question of whether sustained binding underlying stable object representation might be realized, at least in the present case, by synchronous neural activity in the theta frequency band concurrent with suppression of the beta band.

Prediction (3): Decay of gamma activity prior to perceptual reversals. Psychophysical and physiological evidence suggests that an initially stable conscious percept gradually wanes up to an instant of maximal instability, after which an alternative object representation is built up (e.g., Long, Toppino, & Mondin, 1992; Roeber & Vesper, 2009; Strüber & Herrmann, 2002). Accordingly, gamma activity should decrease slowly prior to endogenous reversals and collapse suddenly in the case of exogenously induced reversals.

Psychophysical evidence for decay processes preceding perceptual reversals recently was found by Roeber and Vesper (2009) and Alais, Cass, O'Shea, and Blake (2009). In an MEG experiment with the Stroposcopic Alternative Motion (SAM) stimulus,⁴ Strüber and Herrmann (2002) observed a slow decay of oscillatory activity during endogenous motion reversals and a fast drop after onset in the case of exogenously induced motion reversals of an unambiguous SAM variant. However, this finding pertained to the alpha band and not to the gamma band commonly regarded as relevant for object representation.

Inspection of Figure 3 indicates that, on average, alpha activity decays from the penultimate ([- 1600, - 400] ms) to the last segment ([- 400, 800] ms) before the key press, in agreement with Strüber and Herrmann's results. Notably, this pattern is restricted neither to the unambiguous stimuli nor to the reversal condition. In fact, the overall shapes of the band activity traces BAT_{grand} in the lower frequency bands exhibit a number of striking similarities. Such are prominent when comparing (1) the BAT_{grand} across stimuli and conditions (theta, alpha, beta), (2) the respective time courses within the penultimate and the last segment before the key press (theta; in the alpha and beta bands up to an overall downward shift), and (3) the BAT_{grand} for the alpha and beta bands (apart from the difference in magnitude of the amplitude deflections). Initially, this homogeneity—which also prevails at electrodes other than P4 and Cz (not shown in Figure 3)—renders it unlikely that oscillations in the lower frequency bands (theta, alpha, beta) should carry important information specific to stimulus type or to perceptual reversal/stability. They rather may reflect processes triggered by the discontinuous presentation mode and slow state changes across time.

The slow/fast decay phenomenon initially was hypothesized to occur in the gamma frequency range. Close examination of Figure 3 suggests that, in the reversal condition, the BAT_{grand}

decay after stimulus onset (at $t = 0$) in the range 26–40 Hz may indeed be steeper at electrode Cz for the unambiguous than for the ambiguous stimulus. However, the evidence is weak.

Individual versus Group Results

Most of the time–frequency components determined on the basis of grand means could also be found in individuals, though generally for a few only, and for different ones—maximally 4 out of 16 in the case of component A1 (Table 2). The reasons behind this gap can be manifold. In the best case, the trial-wise variability within participants is too large to allow for individual significance, but effects are homogeneous enough across participants to aggregate to population-wise significance. The latter may, however, also be due to the influence of a single subject and vanish if it is excluded from the population. Such is the case with component A4, for instance, where three-significance is missed upon exclusion of 1 of the 16 participants, even if the criterion is weakened to $p < .1$ for all baselines.

On a more fundamental note, grand average analyses certainly are appropriate if effects for the single participants are weak but unanimous, described as the best case above. However, they appear less appropriate if response patterns are dissimilar or oppositional across participants. Sometimes such may result from artifacts and can safely be ignored. Pattern classification would account for diversity but does not give way to one-sentence take-home messages. A purely statistical approach would declare deviant cases as outliers and focus on the bulk. In fact, at the lower sensory or motor processing levels, all human brains seem to work similarly, which affords the basis for neurological diagnostics. Here, the statistical approach appears suitable. However, the more cognitive neural processing becomes, the more likely it is that individuality prevails over commonness. From this perspective, interindividual discrepancies present less surprise than the often remarkable similarities of grand averages across different conditions, a circumstance that allows differential analyses to focus on a few components only.

Does Gamma Predict Spontaneous Perceptual Reversals?

The most conspicuous and robust result of our study was the pattern of increased and decreased gamma activity in the inter-stimulus interval preceding those ambiguous stimuli that were indicated as reversed. No such effects were observed in the case of unambiguous stimuli. Additional evidence from other studies indicates that this increase of right-hemispheric induced gamma activity at about 200 ms before onset and its subsequent occipital/parietal decrease may be highly specific to and even predictive for endogenous reversals.

Thus Başar-Eroglu et al. (1996) reported a right anterior gamma increase during endogenous perceptual reversals of the SAM stimulus. VanRullen et al. (2006) recently found higher gamma activity at right hemispheric central locations with illusory motion direction reversals of the Wagon-Wheel Illusion compared to real motion reversals. Lumer, Friston, and Rees (1998) found selective right hemispheric functional magnetic resonance imaging (fMRI) activation during perceptual transitions of binocular rivalry stimuli, but no such activity with exogenous transitions of unambiguous stimulus variants. Sterzer and Kleinschmidt (2007) reported an increased fMRI response in the right inferior frontal cortex with endogenous motion reversals of the SAM stimulus compared to exogenously induced reversals of unambiguous SAM variants. Similarly, Ilg et al. (2008) found posterior right hemispheric fMRI activity with spontaneous

⁴The SAM stimulus was introduced by von Schiller (1933) and consists of four dots placed at the corners of an imaginary square. Two diagonal dots flash together in synchrony and in alternation with the other diagonal pair. This presentation mode induces either apparent horizontal or vertical motion. Both directions of motion perception are mutually exclusive, instable, and alternate spontaneously with each other.

motion direction reversals of the spinning wheel illusion (Wertheimer, 1912), but no such activity with exogenously induced reversals. Roeber et al. (2008) recently reported a right hemispheric ERP correlate of binocular rivalry of sine wave gratings. Muller et al. (2005) used the onset of the SAM stimulus immediately before a button press as the time reference for reversals of motion direction. They found changes in EEG activity about 300 ms before the reversal-related SAM flashes, that is, temporally close to our pre-onset gamma modulation. Spatial information was not provided. Britz et al. (2009) reported right-hemispheric EEG correlates anticipating spontaneous perceptual reversals. They used the same onset paradigm and type of ambiguous stimulus as in the present work, but did not consider unambiguous stimulus variants. In summary, all studies listed above reported right-hemispheric EEG activity accompanying endogenous perceptual reversals. Some of them provide a sufficient temporal resolution to locate this activity prior to endogenous reversals.

Conclusions

Single-cell recordings in primates and MEG studies in humans indicate that stable object representation is accompanied by sustained oscillatory activity in the gamma frequency range (e.g., Tallon-Baudry, 2009). In contrast, in the present study with EEG data, the periods of perceptual stability were

accompanied by a sustained increase of theta and decrease of beta activity. iGBA was transient only, as in many other EEG studies, and was delayed by more than 100 ms compared to the onset of lower frequency oscillations (beta, theta). The delay casts doubt on iGBA as a correlate of binding processes as understood here, which should begin early after stimulus onset. On the other hand, (differential) iGBA also could not be reduced to miniature saccades. Thus the role of the post-onset gamma modulations remains largely unclear in the present study.

Transient right-hemispheric modulations of gamma activity were found in the interstimulus interval preceding an endogenous perceptual reversal by about 200 ms. Remarkably, similar prereversal right-hemispheric activations were observed with a variety of paradigms and ambiguous stimuli. A common feature of all these settings is spontaneous perceptual reversals and, along with them, endogenously generated transitions from one stable brain state to another. We speculate that prereversal gamma modulations might reflect a transient brain state of maximal instability reached in the interstimulus interval antedating a perceptual reversal or else the recognition of that state by some unconscious and so far unknown neural instance.

REFERENCES

- Alais, D., Cass, J., O'Shea, R. P., & Blake, R. (2009). Adaptation-related changes during binocular rivalry phases: Dominance sensitivity declines, suppression sensitivity improves. *Perception*, *38*, 1–4.
- American Clinical Neurophysiology Society. (2006). Guideline 5: Guidelines for standard electrode position nomenclature. *Journal of Clinical Neurophysiology*, *23*, 107–110.
- Başar-Eroglu, C., Strüber, D., Schürmann, M., Stadler, M., & Başar, E. (1996). Gamma-band responses in the brain: A short review of psychophysiological correlates and functional significance. *International Journal of Psychophysiology*, *24*, 101–112.
- Blake, R., & Logothetis, N. K. (2002). Visual competition. *Nature Reviews Neuroscience*, *3*, 13–21.
- Borisyuk, R., Chik, D., & Kazanovich, Y. (2009). Visual perception of ambiguous figures: Synchronization based neural models. *Biological Cybernetics*, *100*, 491–504.
- Britz, J., Landis, T., & Michel, C. M. (2009). Right parietal brain activity precedes perceptual alternation of bistable stimuli. *Cerebral Cortex*, *19*, 55–65.
- Cosmelli, D., David, O., Lachaux, J. P., Martinerie, J., Garnero, L., Renault, B., et al. (2004). Waves of consciousness: Ongoing cortical patterns during binocular rivalry. *NeuroImage*, *23*, 128–140.
- Doesburg, S. M., Kitajo, K., & Ward, L. M. (2005). Increased gamma-band synchrony precedes switching of conscious perceptual objects in binocular rivalry. *NeuroReport*, *16*, 1139–1142.
- Eckhorn, R., Bauer, R., Jordan, W., Brosch, M., Kruse, W., Munk, M., et al. (1988). Coherent oscillations: A mechanism of feature linking in the visual cortex? Multiple electrode and correlation analyses in the cat. *Biological Cybernetics*, *60*, 121–130.
- Edgington, E. S., & Onghena, P. (2007). *Randomization Tests* (4th ed). Boca Raton, FL: Chapman & Hall/CRC.
- Engel, A. K., Fries, P., Konig, P., Brecht, M., & Singer, W. (1999). Temporal binding, binocular rivalry, and consciousness. *Consciousness and Cognition*, *8*, 128–151.
- Engel, A. K., Fries, P., & Singer, W. (2001). Dynamic predictions: Oscillations and synchrony in top-down processing. *Nature Reviews Neuroscience*, *2*, 704–716.
- Fries, P., Nikolic, D., & Singer, W. (2007). The gamma cycle. *Trends in Neurosciences*, *30*, 309–316.
- Fries, P., Roelfsema, P. R., Engel, A. K., Konig, P., & Singer, W. (1997). Synchronization of oscillatory responses in visual cortex correlates with perception in interocular rivalry. *Proceedings of the National Academy of Sciences, USA*, *94*, 12699–12704.
- Fries, P., Schroder, J. H., Roelfsema, P. R., Singer, W., & Engel, A. K. (2002). Oscillatory neuronal synchronization in primary visual cortex as a correlate of stimulus selection. *Journal of Neuroscience*, *22*, 3739–3754.
- Gail, A., Brinksmeier, H. J., & Eckhorn, R. (2004). Perception-related modulations of local field potential power and coherence in primary visual cortex of awake monkey during binocular rivalry. *Cerebral Cortex*, *14*, 300–313.
- Gray, C. M., Konig, P., Engel, A. K., & Singer, W. (1989). Oscillatory responses in cat visual cortex exhibit inter-columnar synchronization which reflects global stimulus properties. *Nature*, *338*, 334–337.
- Herrmann, C. S., Munk, M. H., & Engel, A. K. (2004). Cognitive functions of gamma-band activity: Memory match and utilization. *Trends in Cognitive Sciences*, *8*, 347–355.
- Hirabayashi, T., & Miyashita, Y. (2005). Dynamically modulated spike correlation in monkey inferior temporal cortex depending on the feature configuration within a whole object. *Journal of Neuroscience*, *25*, 10299–10307.
- Hoogenboom, N., Schoffelen, J. M., Oostenveld, R., Parkes, L. M., & Fries, P. (2006). Localizing human visual gamma-band activity in frequency, time and space. *NeuroImage*, *29*, 764–773.
- Ilg, R., Wohlschläger, A. M., Burazanis, S., Woller, A., Nunnemann, S., & Muhlau, M. (2008). Neural correlates of spontaneous percept switches in ambiguous stimuli: An event-related functional magnetic resonance imaging study. *European Journal of Neuroscience*, *28*, 2325–2332.
- İşoğlu-Alkaç, Ü., Başar-Eroglu, C., Ademoglu, A., Demiralp, T., Miener, M., & Stadler, T. (2000). Alpha activity decreases during the perception of Necker cube reversals: An application of wavelet transform. *Biological Cybernetics*, *82*, 313–320.
- Keil, A., Muller, M. M., Ray, W. J., Gruber, T., & Elbert, T. (1999). Human gamma band activity and perception of a gestalt. *Journal of Neuroscience*, *19*, 7152–7161.
- Kirchner, H., & Thorpe, S. J. (2006). Ultra-rapid object detection with saccadic eye movements: Visual processing speed revisited. *Vision Research*, *46*, 1762–1776.
- Klimesch, W., Freunberger, R., Sauseng, P., & Gruber, W. (2008). A short review of slow phase synchronization and memory: Evidence for

- control processes in different memory systems? *Brain Research*, 1235, 31–44.
- Koch, S. P., Werner, P., Steinbrink, J., Fries, P., & Obrig, H. (2009). Stimulus-induced and state-dependent sustained gamma activity is tightly coupled to the hemodynamic response in humans, 29, 13962–13970.
- Kornmeier, J., & Bach, M. (2004). Early neural activity in Necker-cube reversal: Evidence for low-level processing of a gestalt phenomenon. *Psychophysiology*, 41, 1–8.
- Kornmeier, J., & Bach, M. (2005). The Necker cube—An ambiguous figure disambiguated in early visual processing. *Vision Research*, 45, 955–960.
- Kornmeier, J., & Bach, M. (2006). Bistable perception—Along the processing chain from ambiguous visual input to a stable percept. *International Journal of Psychophysiology*, 62, 345–349.
- Kornmeier, J., Heinrich, S. P., Atmanspacher, H., & Bach, M. (2001). The reversing “Necker Wall”—A new paradigm with reversal entrainment reveals an early EEG correlate. Paper presented at the ARVO 2001 Annual Meeting, Fort Lauderdale, Florida, USA.
- Livingstone, M., & Hubel, D. (1988). Segregation of form, color, movement, and depth: Anatomy, physiology, and perception. *Science*, 240, 740–749.
- Long, G. M., & Toppino, T. C. (2004). Enduring interest in perceptual ambiguity: Alternating views of reversible figures. *Psychological Bulletin*, 130, 748–768.
- Long, G. M., Toppino, T. C., & Mondin, G. W. (1992). Prime time: Fatigue and set effects in the perception of reversible figures. *Perception & Psychophysics*, 52, 609–616.
- Lumer, E. D., Friston, K. J., & Rees, G. (1998). Neural correlates of perceptual rivalry in the human brain. *Science*, 280, 1930–1934.
- Lutzenberger, W., Pulvermüller, F., Elbert, T., & Birbaumer, N. (1995). Visual stimulation alters local 40-Hz responses in humans: An EEG study. *Neuroscience Letters*, 183, 39–42.
- Mathes, B., Strüber, D., Stadler, M. A., & Basar-Eroglu, C. (2006). Voluntary control of Necker cube reversals modulates the EEG delta- and gamma-band response. *Neuroscience Letters*, 402, 145–149.
- Milner, P. M. (1974). A model for visual shape recognition. *Psychological Review*, 81, 521–535.
- Muller, T. J., Federspiel, A., Fallgatter, A. J., & Strik, W. K. (1999). EEG signs of vigilance fluctuations preceding perceptual flips in multistable illusory motion. *NeuroReport*, 10, 3423–3427.
- Muller, T. J., Koenig, T., Wackermann, J., Kalus, P., Fallgatter, A., Strik, W., et al. (2005). Subsecond changes of global brain state in illusory multistable motion perception. *Journal of Neural Transmission*, 112, 565–576.
- Necker, L. A. (1832). Observations on some remarkable optical phaenomena seen in Switzerland; and on an optical phaenomenon which occurs on viewing a figure of a crystal or geometrical solid. *London and Edinburgh Philosophical Magazine and Journal of Science*, 1, 329–337.
- Orbach, J., Ehrlich, D., & Heath, H. (1963). Reversibility of the Necker cube: I. An examination of the concept of “satiation of orientation”. *Perceptual and Motor Skills*, 17, 439–458.
- Orbach, J., Zucker, E., & Olson, R. (1966). Reversibility of the Necker cube: VII. Reversal rate as a function of figure-on and figure-off durations. *Perceptual and Motor Skills*, 22, 615–618.
- Papoulis, A. (1962). *The Fourier integral and its applications*. New York: McGraw-Hill.
- Pfurtscheller, G., & Lopes da Silva, F. H. (1999). Event-related EEG/MEG synchronization and desynchronization: Basic principles. *Clinical Neurophysiology*, 110, 1842–1857.
- Pitts, M. A., Neger, J. L., & Davis, T. J. R. (2007). Electrophysiological correlates of perceptual reversals for three different types of multistable images. *Journal of Vision*, 7, 1–14.
- Revonsuo, A. (1999). Binding and the phenomenal unity of consciousness. *Consciousness and Cognition*, 8, 173–185.
- Roeber, U., & Veser, S. (2009). Depth of binocular-rivalry suppression reduces with time of suppression: Electrophysiological evidence. *Perception*, 38(suppl.), 154.
- Roeber, U., Widmann, A., Trujillo-Barreto, N. J., Herrmann, C. S., O’Shea, R. P., & Schröger, E. (2008). Early correlates of visual awareness in the human brain: Time and place from event-related brain potentials. *Journal of Vision*, 8, 1–12.
- Rolls, E. T. (2000). Memory systems in the brain. *Annual Review of Psychology*, 51, 599–630.
- Roskies, A. L. (1999). The binding problem. *Neuron*, 247–9, 111–125.
- Schroeder, C. E., & Lakatos, P. (2009). The gamma oscillation: Master or slave? *Brain Topography*, 22, 24–26.
- Shadlen, M. N., & Movshon, J. A. (1999). Synchrony unbound: A critical evaluation of the temporal binding hypothesis. *Neuron*, 2467–77, 111–25.
- Sterzer, P., & Kleinschmidt, A. (2007). A neural basis for inference in perceptual ambiguity. *Proceedings of the National Academy of Sciences, USA*, 104, 323–328.
- Sterzer, P., & Rees, G. (2008). A neural basis for percept stabilization in binocular rivalry. *Journal of Cognitive Neuroscience*, 20, 389–399.
- Strüber, D., Basar-Eroglu, C., Hoff, E., & Stadler, M. (2000). Reversal-rate dependent differences in the EEG gamma-band during multistable visual perception. *International Journal of Psychophysiology*, 38, 243–252.
- Strüber, D., Basar-Eroglu, C., Miener, M., & Stadler, M. (2001). EEG gamma-band response during the perception of Necker cube reversals. *Visual Cognition*, 8, 609–621.
- Strüber, D., & Herrmann, C. S. (2002). MEG alpha activity decrease reflects destabilization of multistable percepts. *Cognitive Brain Research*, 14, 370–382.
- Tallon-Baudry, C. (2009). The roles of gamma-band oscillatory synchrony in human visual cognition. *Frontiers in Bioscience*, 14, 321–332.
- Tallon-Baudry, C., & Bertrand, O. (1999). Oscillatory gamma activity in humans and its role in object representation. *Trends in Cognitive Science*, 3, 151–162.
- Tallon-Baudry, C., Bertrand, O., Henaff, M. A., Isnard, J., & Fischer, C. (2005). Attention modulates gamma-band oscillations differently in the human lateral occipital cortex and fusiform gyrus. *Cerebral Cortex*, 15, 654–662.
- Treisman, A., & Gormican, S. (1988). Feature analysis in early vision: Evidence from search asymmetries. *Psychological Review*, 95, 15–48.
- Uhlhaas, P. J., Pipa, G., Lima, B., Melloni, L., Neuenschwander, S., Nikolicevic, D., et al. (2009). Neural synchrony in cortical networks: History, concept and current status. *Frontiers in Integrative Neuroscience*, 3, 17.
- VanRullen, R., Reddy, L., & Koch, C. (2006). The continuous wagon wheel illusion is associated with changes in electroencephalogram power at approximately 13 Hz. *Journal of Neuroscience*, 26, 502–507.
- Varela, F., Lachaux, J. P., Rodriguez, E., & Martinerie, J. (2001). The brainweb: Phase synchronization and large-scale integration. *Nature Reviews Neuroscience*, 2, 229–239.
- von der Malsburg, C. (1981). *The correlation theory of brain function*. Internal Report No. 81-2. Göttingen, Germany: Max-Planck-Institut für biophysikalische Chemie.
- von Schiller, P. (1933). Stroboskopische Alternativversuche. *Psychologische Forschung*, 17, 179–214.
- Wertheimer, M. (1912). Experimentelle Studien über das Sehen von Bewegungen. *Zeitschrift für Psychologie*, 61, 161–265.
- Woo, M., Neider, J., & Davis, T. (1998). *OpenGL Programming Guide. The Official Guide to learning OpenGL, Version 1.1* (2nd ed). Reading, MA: Addison-Wesley.
- World Medical Association. (2000). Declaration of Helsinki: Ethical principles for medical research involving human subjects. *Journal of the American Medical Association*, 284, 3043–3045.
- Yuval-Greenberg, S., & Deouell, L. Y. (2009). The broadband-transient induced gamma-band response in scalp EEG reflects the execution of saccades. *Brain Topography*, 22, 3–6.
- Yuval-Greenberg, S., Tomer, O., Keren, A. S., Nelken, I., & Deouell, L. Y. (2008). Transient induced gamma-band response in EEG as a manifestation of miniature saccades. *Neuron*, 58, 429–441.

(RECEIVED January 20, 2010; ACCEPTED June 11, 2010)